# MYPT1 O-GlcNAcylation Dictates Timely Disjunction of Centrosomes

**Caifei Liu[1,*], Yingxin Shi[1,*], Xuewen Liu[2], Zhikai Xiahou[2], Jie Li[1] , Zhongping Tan[3], Xing Chen[4] and Jing Li[1, §]**

[1]Beijing Key Laboratory of DNA Damage Response and College of Life Sciences, Capital Normal University, Beijing 100048, China

[2]Department of Radiation Oncology, Hunan Cancer Hospital and The Affiliated Cancer Hospital of Xiangya School of Medicine, Central South University, Changsha, PR China; Key Laboratory of Translational Radiation Oncology, Hunan 410006, China

[3] Institute of Materia Medica, Chinese Academy of Medical Sciences and Peking Union Medical College, Beijing, 100050, China.

[4]College of Chemistry and Molecular Engineering, Beijing National Laboratory for Molecular Sciences, Peking-Tsinghua Center for Life Sciences, Synthetic and Functional Biomolecules Center, and Key Laboratory of Bioorganic Chemistry and Molecular Engineering of Ministry of Education, Peking University, Beijing 100871, China.

Running title: O-GlcNAc of MYPT1 regulates centrosome dynamics

[*]These authors contributed equally to this work.

**[§]To whom correspondence should be addressed:**

Jing Li, [1]Beijing Key Laboratory of DNA Damage Response, College of Life Sciences, Capital Normal University, Beijing 100048, China, Phone: 86-10-68901692, Fax: 86-10-68906307, E-mail:jing_li@mail.cnu.edu.cn

Keywords : O-GlcNAcylation; O-linked N-acetylglucosamine (O-GlcNAc) transferase (OGT); O-linked N-acetylglucosamine (O-GlcNAc); MYPT1 ; cell cycle ; mitosis ; protein phosphorylation ; CDK1 ; PLK1 ; centrosome

## ABSTRACT

The role of O-linked N-acetylglucosamine (O-GlcNAc) modification in the cell cycle has been enigmatic. Previously, both O-GlcNAc transferase (OGT) and O-GlcNAcase (OGA) disruption have been shown to derail the mitotic centrosome numbers, suggesting that mitotic O-GlcNAc oscillation needs to be in concert with mitotic progression to account for centrosome integrity. Here we attempted to address the underlying molecular mechanism by both chemical approaches and biological assays, and observed that Thiamet-G (OGA inhibitor) incubation strikingly elevated centrosomal distances, suggestive of premature centrosome disjuction. These aberrancies could be overcome by inhibiting Polo-like kinase 1 (Plk1), a mitotic master kinase. Plk1 inactivation is modulated by the Myosin Phosphatase Targeting Subunit 1 (MYPT1)-Protein Phosphatase 1 cβ (PP1cβ) complex. Interestingly, MYPT1 is abundantly O-GlcNAcylated and the modified residues have been detected in a recent O-GlcNAc profiling screen utilizing chemoenzymatic labeling and bioorthogonal conjugation. We demonstrate that MYPT1 is O-GlcNAcylated at T577, S585, S589 and S601, which antagonizes CDK1-dependent phosphorylation at S473, subsequently attenuating the association between MYPT1 and Plk1, and promoting PLK1 activity. Thus under high O-GlcNAc, Plk1 is untimely activated, conducive to inopportune centrosome separation and disrupting the cell cycle. We propose that too much O-GlcNAc is equally deleterious as too little O-GlcNAc, and a fine balance between the OGT/OGA duo is indispensible for successful mitotic divisions.

## INTRODUCTION

The centrosomes are the primary microtubule-organizing centers that nucleate the mitotic spindle apparatus to ensure subsequent faithful sister chromatid segregation during mitosis. The centrosome cycle is tightly coordinated with other cell cycle events [1], and its aberrancy could culminate in chromosome segregation defects and aneuploidy [2]. The entire centrosome cycle encompasses centrosome duplication during S phase, disjunction in late G2 and further separation during prophase or prometaphase, and eventual segregation into the two daughter cells.

Centrosomes duplicate in concomitant with DNA replication, after which the sister centrosomes are glued together by two proteinaceous linkers, c-Nap1 and rootletin [3,4], as well as other components such as Cep68, Cep215 and LRRC45 [5]. C-Nap1, a large coiled-coiled protein, links rootletin to the centrioles so that the centrosome pair is joined by fibrous polymers [3]. In late G2, the Never In Mitosis (NIMA)-related serine/threonine kinase Nek2A phosphorylates and displaces c-Nap1 and rootletin, leading to disjoint centrosomes [6]. Centrosomal accumulation of Nek2A is mediated by the Hippo pathway, among which sterile 20-like kinase 2 (Mst2) and Salvador (Sav1) play critical roles. In particular, Mst2 phosphorylates and activates Nek2A[7]. Upstream of Mst2 is the mitotic master kinase, Polo-like kinase 1 (PLK1) [8].

Following centrosome disjunction, the kinesin Eg5 accounts for centrosome positioning in the beginning of M phase. Cyclin-dependent kinase 1 (Cdk1) phosphorylates and activates Eg5 at T927 by stimulating the engagement between

77 Eg5 and microtubules [9]. Independently, centrosomal localization of Eg5 requires
78 PLK1 [10], which activates the NIMA-family kinase Nek9, leading to Eg5
79 phosphorylation at S1033 by the Nek9/6/7 complex [11]. Phosphorylated Eg5 then binds
80 centrosomal Targeting Protein for Xenopus kinesin-like protein 2 (TPX2), which is
81 also mediated by Nek9 [12]. Besides mitosis, Eg5 also governs centrosome dynamics
82 during interphase [10]. Hence, the centrosomal role of Plk1 is two-fold : centrosome
83 disjunction via the PLK1-Mst2-Nek2A signaling cascade, and centrosome separation
84 through PLK1- Nek9/6/7- Eg5[13].

85 Besides centrosomes, PLK1 also orchestrates a multitude of cell cycle events,
86 including replication, mitotic entry, chromosome segregation and cytokinesis [4,14-16]. It
87 contains an N-terminal kinase domain and a C-terminal polo-box binding domain
88 (PBD). Phosphorylation of PLK1 at T210 at the T-loop is mediated by the Aurora
89 A-Bora complex [17], resulting in dissociation of PBD from the kinase domain and thus
90 activating PLK1. Dephosphorylation of PLK1 is modulated by the protein
91 phosphatase 1 cβ (PP1cβ), targeted by the myosin phosphatase targeting subunit 1
92 (MYPT1) [18]. Specifically, CDK1 phosphorylates MYPT1 at Ser473, creating a
93 binding pocket between MYPT1 and the PBD of PLK1. Subsequently MYPT1
94 recruits PP1cβ to dephosphorylate pT210 of PLK1[18]. Such interaction at the
95 kinetochore destabilizes kinetochore-microtububle attachments [19]. Besides
96 phosphorylation, PLK1 is also methylated at K209 [20,21], which vies with pT210 and
97 hence blocking Plk1 activity.

Due to the vital role of PLK1 in mitosis, MYPT1 is subject to multifaceted regulations: the Hippo pathway kinase LATS1/WARTS phosphorylates MYPT1 at S445 to inactivate PLK1 [22] ; optineurin, another phosphatase, promotes MYPT1 activity [23] ; checkpoint kinase 1 (CHK1) phosphorylates MYPT1 at S20, and enhances MYPT1-PP1cβ binding [24] ; checkpoint kinase 2 (CHK2) phosphorylates MYPT1 at S507 to attenuate pS473 [25].

Previous investigations have identified that MYPT1 is also subject to O-linked N-acetylglucosamine (O-GlcNAc) modifications [26]. O-GlcNAcylation is an emerging post-translational modification (PTM) that integrates the metabolic signals with transcription, nutrient sensing, stress responses and cell cycle events [27,28]. It is catalyzed by the sole transferase O-GlcNAc transferase (OGT), and reversed by the only O-GlcNAcase (OGA) [27]. Chemical inhibitors of OGT [acetyl-5S-GlcNAc (5S-G)] and OGA [Thiamet-G (TMG)] have been developed to interogate various biological processes[29]. During the cell cycle, O-GlcNAcylation levels fluctuate as the cells proceed through different stages [30]. In particular, both OGT and OGA overproduction results in multipolar spindles [31]. However, myriad targets of O-GlcNAc and its quintessential functions remain largely unexplored. Here we identify the O-GlcNAc modified residues of MYPT1. We show that O-GlcNAcylation of MYPT1 antagonizes pS473, and results in its dissociation from PLK1. Elevated O-GlcNAc levels thus fuel PLK1 activity towards centrosomes and render ill-timed centrosome separation, disrupting the mitotic cell cycle.

## RESULTS

### O-GlcNAc promotes aberrant centrosome separation via PLK1

Previously, both OGT and OGA overproduction has been linked with multi-polar spindle [31]. We sought to identify whether O-GlcNAc could also be linked with centrosome dynamics. Strikingly, when HeLa cells were treated with TMG (OGAi), the inter-centrosomal distance was significantly augmented four-fold (Fig. 1A), reminiscent of the phenotype of Nek2A overexpression or over-activation [4,32]. As the centrosome cycle is tightly governed by PLK1, we attempted to inhibit PLK1. When BI2536 (PLK1i) was adopted in conjuncture with TMG, the centrosomal distances shortened considerably (Fig. 1A-C). When BI2536 was utilized alone (Fig. 1A), the cells reduced centrosomal distances as previously reported [4]. These cytological studies suggest that high O-GlcNAc culminates in premature centrosomal separation, probably via PLK1.

### MYPT1 is O-GlcNAcylated at T577, S585, S589 and S601.

Previous investigation has identified the inactivating phosphatase of PLK1 is PP1cβ, which is targeted by MYPT1 [18]. Intriguingly, MYPT1 is O-GlcNAcylated [26]. Therefore we reasoned that O-GlcNAc might exert its effect through MYPT1.

First, we validated the interaction between MYPT1 and OGT through biochemical assays. As shown in Fig. 2A, GST-OGT pulled-down HA-MYPT1 from cell extracts. Then both OGT and MYPT1 proteins were purified from *E. coli*. Upon

incubation, His-OGT pulled-down GST-MYPT1 (Fig. 2B), suggesting that the interact is direct.

Then we mapped which domain of MYPT1 interacts with OGT. As MYPT1 is a relative large protein, we constructed several fragments of MYPT1 as previously described: F1 (1-306), F2 (297-600), F3 (586-901) and F4 (886-1030) (Fig. 2C) [24]. To investigate which fragment interacts with OGT, recombinant full-length (FL) and F1-F4 MYPT1 proteins were utilized in pulldown experiments, and the FL, F2 and F3 MYPT1 pulled-down Myc-OGT (Fig. 2D), suggesting that the potential modification sites could be residing in F2 and F3.

A recent quantitative proteomic analysis of protein O-GlcNAc sites using an isotope-tagged cleavable linker (isoTCL) strategy identified the potential O-GlcNAc sites of MYPT1 to be T577, S585, S589 and S601 [33] (Fig. 3 A-D), all of which locate on F2 and F3. We constructed the T577A/S585A/S589A/S601A (4A) mutant accordingly and assessed its effect. When HA-MYPT1-wild type (WT) and 4A plasmids were transfected into cells, the 4A mutant significantly abrogated O-GlcNAcylation (Fig. 4A), suggesting that these four amino acids are major O-GlcNAc sites. Considering that MYPT1 is abundantly O-GlcNAcylated, and other proteomic screens have also identified extra glycosylation sites [34], our results do not exclude the possibility that there could be more O-GlcNAcylated residues on MYPT1.

**O-GlcNAcylation of MYPT1 antagonizes CDK1-dependent phosphorylation at S473**

Since CDK1 phosphorylates MYPT1 at S473 during mitosis and creates a binding motif between MYPT1 and the PBD of PLK1[18], we surmised that O-GlcNAc of MYPT1 might interplay with pS473. To address this possibility, we used a phospho-specific antibody targeting pS473 that has been previously described and utilized [25].

Then the WT and 4A plasmids are compared for the pS473 levels, and it is significantly bolstered in the 4A mutant (Fig. 4B). When Noc was used to synchronize cells in the M phase, O-GlcNAc levels decreased while pS473 levels arose (Fig. 4C). As pS473 is mediated by CDK1, we adopted RO-3306 again, and observed that RL2 levels decreased while pS473 levels increased in the RO-3306-treated cells (Fig.4C). This is consistent with our conjecture that O-GlcNAc antagonizes pS473. Lastly, we utilized the 5S-G inhibitor for OGT [29], and 5S-G treatment substantially boosted pS473 levels of transfected HA-MYPT1(Fig. 4D). We also examined the effects of 5S-G on endogenous MYPT1. Noc treatment enhanced pS473 levels, and Noc plus 5S-G elevated pS473 markedly (Fig. 4E). In contrast, glucose plus TMG (TMG+Glu) treatment during Noc would down-regulate pS473 compared to Noc alone (Fig. 4F). Taken together, O-GlcNAc of MYPT1 attenuates pS473.

**O-GlcNAcylation inhibits MYPT1-PLK1 association**

Since pS473 promotes MYPT1-PLK1 association [18], we then explored the effect of O-GlcNAc on the interaction between MYPT1 and PLK1 by treating the cells with TMG+Glu to enhance O-GlcNAc [35,36]. As shown in Fig. 5A, Noc increased PLK1-MYPT1 association discernably as reported [18], but TMG+Glu together with Noc obliterated PLK1-MYPT1 affinity.

As phosphorylated MYPT1 binds with PLK1-PBD [18] , we adopted GST pulldown experiments using PLK1-PBD, and GST-PLK1-PBD modestly increased binding with HA-MYPT1-4A (Fig. 5B). Then we employed FL-PLK1. When we directly utilized the 4A mutant to coIP PLK1, the interaction between MYPT1 and PLK1 substantially upregulated (Fig. 5C).When His-PLK1 was applied in pulldown assays, 4A again manifested more robust association with PLK1(Fig. 5D). In sum, the binding between PLK1 and MYPT1 was abolished during high O-GlcNAc.

**O-GlcNAcylation of MYPT1 enhances PLK1 activity**

As the MYPT1 associates PLK1 to target PP1cβ to dephosphorylate and deactivate PLK1 [18], stronger affinity could signify less activity. We took advantage of the IP-phosphatase assay to examine PLK1 activity [22,24]. Cells were transfected with Flag-MYPT1 and treated with Noc. Cells were also supplemented with TMG + Glu to enrich for O-GlcNAc or not treated. When the anti-FLAG immunoprecipitates were incubated with recombinant PLK1, the relative low O-GlcNAc group efficiently

dephosphorylated PLK1, as detected by IB with PLK1-pT210 antibodies, but not the high O-GlcNAc group (Fig. 6A).

MYPT1-4A mutants were then directly exploited in the IP-phosphate assay. In the absence of Noc, MYPT1-WT decreased PLK1 pT210 levels, and the MYPT1-4A completely abolished PLK1-pT210 levels (Fig. 6B). This is consistent with our results in Fig. 5C-D that MYPT1-4A partners with PLK1 in the absence of Noc treatment. Collectively, our biochemical assays suggest that O-GlcNAcylated MYPT1 disjoins PLK1 and promotes its kinase activity.

**MYPT1-4A Suppresses the TMG-induced centrosome disjunction defects**

Since the aforementioned results suggest that MYPT1 O-GlcNAcylation is a pivotal regulator in centrosome separation, we undertook sh*MYPT1* to knockdown endogenous MYPT1 (Fig. 7A), so that the effects of MYPT1-4A could be directly measured and observed after TMG incubation. As shown in Fig. 7B, the premature centrosome separation phenotype is discernable in the sh*MYPT1* cells that bears MYPT1-WT plasmids. But in the cells transfected with MYPT1-4A plasmids, the aberrancy is suppressed (Fig. 7C), in line with previous reports that PLK1 sequestration culminates in duplicated but unseparated centrosomes[37,38]. Taken together, the 4A mutant fails to show the untimely centrosome separation phenotype, probably due to PLK1 suppression.

## DISCUSSION

In this study, we identify that O-GlcNAc regulates centrosome separation through the MYPT1-PLK1 complex. We pinpoint the major O-GlcNAcylated sites of MYPT1 to be S564, S566, T570 and S578 in human cells, and further delineate that O-GlcNAc antagonizes pS473, hinders MYPT1-PLK1 association, thus boosting PLK1 activity and hence centrosome disjunction (Fig. 7D). When MYPT1 fails to be O-GlcNAcylated, as in the MYPT1-4A mutant, PLK1 activity is dampened (Fig. 6B).

MYPT1 is one of the most abundant O-GlcNAcylated proteins, and its modification sites have been unveiled time and again in distinct proteomic studies [34,39,40]. Perhaps O-GlcNAc sites might not be conserved between humans and mice. MYPT1 is found to be O-GlcNAcylated at S564, S566, T570 and S578 by mass spectrometry in the mouse brain [40], but our data show in HeLa cells O-GlcNAc occurs in T577, S585, S589 and S601. Previously, p53 is identified to be O-GlcNAcylated at S149 [41], which is not conserved in mice either. The same also holds true for phosphorylation. For instance, Ataxia-telangiectasia mutated (ATM), a vital sensor protein for DNA damage signaling, is phosphorylated at S1981 and then activated in humans, but mutation of S1987 (the mouse equivalent) does not hinder ATM function in mice[42,43]. Thus extrapolating data across species needs extra caution, as the function and sites of PTMs could be context-dependent.

Along the same vein, there could be more O-GlcNAc sites on MYPT1, as the proteomic studies were carried out under disparate circumstances and using different

click chemistry methodologies [33,34,39,40]. As the O-GlcNAc modification is highly dynamic, distinct sites could be modified in response to environmental cues.

O-GlcNAc could have multi-faceted effects on the centrosome. Both OGT and OGA overexpression result in multi-polar spindles, which could be repressed by TMG treatment [31]. NuMA (nuclear mitotic apparatus protein ) is indispensible for spindle pole formation and regulates spindle pole cohesion [44,45]. NuMA is O-GlcNAcylated and its localization was led astray by OGT overexpression[46]. Further investigations reveal that O-GlcNAcylated NuMA interacts with Galectin-3, which is a prerequisite for mitotic spindle cohesion and proper NuMA localization [47]. Here we reveal that centrosome dynamics is also governed by O-GlcNAcylation levels. As the centrosome is pivotal for the mitotic process, O-GlcNAc is bound to modulate other aspects of centrosome function.

Our results indicate that O-GlcNAcylated MYPT1 attenuates interaction with PLK1 and thus promotes PLK1 activity. It is intriguing that overall PLK1 pT210 levels remain unaltered in OGT or OGA overproduction cells [31,46]. We did not detect discernable difference either, in cells supplemented with TMG plus Glucose (data not shown). This may seem paradoxical at first, but considering the versatile roles of PLK1 during mitosis [4,14-16], we could entertain the possibility that only a small pool of PLK1 is regulated by MYPT1. First, although the overall activity of PLK1 is upregulated during mitosis, CDK1 actually dampens PLK1 activity via MYPT1 in a mitosis-specific fashion [18]. Secondly, the pool of PLK1 responsible for

kinetochore-microtubule attachment actually contains low PLK1 kinase activity during metaphase so that microtubules could be dynamic [48]. Therefore, irrespective of the overall elevation of mitotic activity, the mitotic master kinase - PLK1 is perhaps indeed fine-tuned in space and time. And O-GlcNAc, could be the sweet icing on the cake.

## EXPERIMENTAL PROCEDURES

*Cell culture, antibodies and plasmids*

Cells were purchased from ATCC. Antibodies were as follows: anti-MYPT1 (Bethyl, # BL3866) , anti-PLK1 (Zymed, #37-7100), PLK1-pT210 (BD Pharmingen, #558400). Antibodies against pS473 were prepared as described before [25] and manufactured by Beijing B&M Biotech Co., Ltd.. *MYPT1* plasmids were described before [49]. *MYPT1-4A* plasmids were generated using specific primers (sequences available upon request) following the manufacturer's instructions (QuickChange II, Stratagene). His-OGT was from Dr. Yue Wang (Peking Univ.). The following shRNA target sequences were used: sh*MYPT1:* GTAACCCAGTGGACCATAATT.

*Immunoprecipitation (IP) and Immunoblotting (IB) assays*

IP and IB experiments were performed as described before [50]. The following primary antibodies were used for IB: anti-β-actin (1:10000), anti-HA (1:1000), and anti-FLAG M2 (Sigma) (1:1000), anti-Myc (1:1000), anti-PLK1 (1:1000),

anti-MYPT1 (1:1000), PLK1-pT210 (1:500). The IP-phosphatase assay was performed as before [22,24].

Peroxidase-conjugated secondary antibodies were from JacksonImmuno Research. Blotted proteins were visualized using the ECL detection system (Amersham). Signals were detected by a LAS-4000, and quantitatively analyzed by densitometry using the Multi Gauge software (Fujifilm). All western blots were repeated for at least three times.

*Cell Culture Treatment*

Chemical utilization: Nocodazole (Noc) at 100 ng/ml for 16 hours; Ro 3306 (CDK1 inhibitor) at 2 μM for the time indicated; BI2536 (PLK1 inhibitor) at 100 nM for two hours; Thiamet-G (TMG) (OGA inhibitor) at 5μM for 24 hrs ; acetyl-5S-GlcNAc (5S-G) (OGT inhibitor) was used at 100μM (prepared at 50 mM in DMSO) for 24 hrs [64].

*Indirect Immunofluorescence*

Indirect immunofluorescence staining was performed as described before [50]. Dilutions of primary antibodies were 1:1,000 for mouse anti-γ-tubulin. Cell nuclei were stained with DAPI. Quantitation was performed with the software Image J.

**Abbreviations:**

PTM, post-translational modification; O-GlcNAc, O-linked N-acetylglucosamine; OGT, O-GlcNAc transferase; TMG, Thiamet-G; PBD, polo-box binding domain ; MYPT1, myosin phosphatase targeting subunit 1; Cdk1, Cyclin-dependent kinase 1 ; PLK1, Polo-like kinase 1 ; 5S-G, acetyl-5S-GlcNAc; PP1cβ, protein phosphatase 1 c β ; FL, full-length ; ETD, Electron Transfer Dissociation

**Acknowledgements**

We thank Dr. Hai-Ning Du (Wuhan Univ.) and the Li laboratory for helpful discussion. This work is supported by the National Natural Science Foundation of China (NSFC) fund (31872720) and Capacity Building for Sci-Tech Innovation - Fundamental Scientific Research Funds (19530050137) to J. L.; NSFC (NOs. 21425204, 21672013 and 21521003) and the National Key Research and Development Projects (NOs. 2016YFA0501500 and 2018YFA0507600) to X.C.; NSFC (91853120) and the National Major Scientific and Technological Special Project of China for "Significant New Drugs Development" (2018ZX09711001-013) to Z. T.

**Competing interests**

The authors declare that they have no conflicts of interest with the contents of this article.

## Author contributions

J. L., X.C. and Z.T. conceived the project and analyzed the data. C. L., Y. S., X. L., Z. X. and Jie L. performed all the experiments. All authors reviewed and approved the manuscript.

## References


1 Vertii, A., Hehnly, H. & Doxsey, S. The Centrosome, a Multitalented Renaissance Organelle. *Cold Spring Harb Perspect Biol* **8**, doi:10.1101/cshperspect.a025049 (2016).

2 Silkworth, W. T., Nardi, I. K., Paul, R., Mogilner, A. & Cimini, D. Timing of centrosome separation is important for accurate chromosome segregation. *Mol Biol Cell* **23**, 401-411, doi:10.1091/mbc.E11-02-0095 (2012).

3 Bahe, S., Stierhof, Y. D., Wilkinson, C. J., Leiss, F. & Nigg, E. A. Rootletin forms centriole-associated filaments and functions in centrosome cohesion. *J Cell Biol* **171**, 27-33, doi:10.1083/jcb.200504107 (2005).

4 Mardin, B. R., Agircan, F. G., Lange, C. & Schiebel, E. Plk1 controls the Nek2A-PP1gamma antagonism in centrosome disjunction. *Curr Biol* **21**, 1145-1151, doi:10.1016/j.cub.2011.05.047 (2011).

5 van Ree, J. H., Nam, H. J. & van Deursen, J. M. Mitotic kinase cascades orchestrating timely disjunction and movement of centrosomes maintain chromosomal stability and prevent cancer. *Chromosome Res* **24**, 67-76, doi:10.1007/s10577-015-9501-9 (2016).

6 Hardy, T. *et al.* Multisite phosphorylation of C-Nap1 releases it from Cep135 to trigger centrosome disjunction. *J Cell Sci* **127**, 2493-2506, doi:10.1242/jcs.142331 (2014).

7 Mardin, B. R. *et al.* Components of the Hippo pathway cooperate with Nek2 kinase to regulate centrosome disjunction. *Nat Cell Biol* **12**, 1166-1176, doi:10.1038/ncb2120 (2010).

8 Barr, F. A., Sillje, H. H. & Nigg, E. A. Polo-like kinases and the orchestration of cell division. *Nat. Rev. Mol. Cell. Biol.* **5**, 429-440, doi:10.1038/nrm1401 (2004).

9 Blangy, A. *et al.* Phosphorylation by p34cdc2 regulates spindle association of human Eg5, a kinesin-related motor essential for bipolar spindle formation in vivo. *Cell* **83**, 1159-1169 (1995).

10 Smith, E. *et al.* Differential control of Eg5-dependent centrosome separation by Plk1 and Cdk1. *EMBO J* **30**, 2233-2245, doi:10.1038/emboj.2011.120 (2011).

11 Bertran, M. T. *et al.* Nek9 is a Plk1-activated kinase that controls early centrosome separation through Nek6/7 and Eg5. *EMBO J* **30**, 2634-2647, doi:10.1038/emboj.2011.179 (2011).

12 Eibes, S. *et al.* Nek9 Phosphorylation Defines a New Role for TPX2 in Eg5-Dependent Centrosome Separation before Nuclear Envelope Breakdown. *Curr Biol* **28**, 121-129 e124, doi:10.1016/j.cub.2017.11.046 (2018).

13 Wang, G., Jiang, Q. & Zhang, C. The role of mitotic kinases in coupling the centrosome cycle with the assembly of the mitotic spindle. *J Cell Sci* **127**, 4111-4122, doi:10.1242/jcs.151753 (2014).

14 Zitouni, S., Nabais, C., Jana, S. C., Guerrero, A. & Bettencourt-Dias, M. Polo-like kinases: structural variations lead to multiple functions. *Nat Rev Mol Cell Biol* **15**, 433-452, doi:10.1038/nrm3819 (2014).

15 Song, B., Liu, X. S. & Liu, X. Polo-like kinase 1 (Plk1): an Unexpected Player in DNA Replication. *Cell division* **7**, 3, doi:10.1186/1747-1028-7-3 (2012).

16 Li, J., Wang, J., Jiao, H., Liao, J. & Xu, X. Cytokinesis and cancer: Polo loves ROCK'n' Rho(A). *J. Genet. Genomics.* **37**, 159-172, doi:10.1016/S1673-8527(09)60034-5 (2010).

17 Seki, A., Coppinger, J. A., Jang, C. Y., Yates, J. R. & Fang, G. Bora and the kinase Aurora A cooperatively activate the kinase Plk1 and control mitotic entry. *Science* **320**, 1655-1658, doi:10.1126/science.1157425 (2008).

18 Yamashiro, S. *et al.* Myosin phosphatase-targeting subunit 1 regulates mitosis by antagonizing polo-like kinase 1. *Dev. Cell* **14**, 787-797, doi:10.1016/j.devcel.2008.02.013 (2008).

19 Dumitru, A. M. G., Rusin, S. F., Clark, A. E. M., Kettenbach, A. N. & Compton, D. A. Cyclin A/Cdk1 modulates Plk1 activity in prometaphase to regulate kinetochore-microtubule attachment stability. *Elife* **6**, doi:10.7554/eLife.29303 (2017).

20 Feldman, M., Vershinin, Z., Goliand, I., Elia, N. & Levy, D. The methyltransferase SETD6 regulates Mitotic progression through PLK1 methylation. *Proc Natl Acad Sci U S A* **116**, 1235-1240, doi:10.1073/pnas.1804407116 (2019).

21 Li, W. *et al.* A methylation-phosphorylation switch determines Plk1 kinase activity and function in DNA damage repair. *Sci Adv* **5**, eaau7566, doi:10.1126/sciadv.aau7566 (2019).

22 Chiyoda, T. *et al.* LATS1/WARTS phosphorylates MYPT1 to counteract PLK1 and regulate mammalian mitotic progression. *J Cell Biol* **197**, 625-641, doi:10.1083/jcb.201110110 (2012).

23 Kachaner, D. *et al.* Plk1-dependent phosphorylation of optineurin provides a negative feedback mechanism for mitotic progression. *Mol Cell* **45**, 553-566, doi:10.1016/j.molcel.2011.12.030 (2012).

24 Hu, X. *et al.* Chk1 modulates the interaction between myosin phosphatase targeting protein 1 (MYPT1) and protein phosphatase 1cbeta (PP1cbeta). *Cell Cycle* **17**, 421-427, doi:10.1080/15384101.2017.1418235 (2018).

25 Nai, S. *et al.* Chk2-dependent phosphorylation of myosin phosphatase targeting subunit 1 (MYPT1) regulates centrosome maturation. *Cell Cycle*, 1-9, doi:10.1080/15384101.2019.1654795 (2019).

26 Cheung, W. D., Sakabe, K., Housley, M. P., Dias, W. B. & Hart, G. W. O-linked beta-N-acetylglucosaminyltransferase substrate specificity is regulated by myosin phosphatase targeting and other interacting proteins. *J Biol Chem* **283**, 33935-33941, doi:10.1074/jbc.M806199200 (2008).

27 Hart, G. W., Slawson, C., Ramirez-Correa, G. & Lagerlof, O. Cross talk

between O-GlcNAcylation and phosphorylation: roles in signaling, transcription, and chronic disease. *Annu Rev Biochem* **80**, 825-858, doi:10.1146/annurev-biochem-060608-102511 (2011).

28 Yang, X. & Qian, K. Protein O-GlcNAcylation: emerging mechanisms and functions. *Nat Rev Mol Cell Biol* **18**, 452-465, doi:10.1038/nrm.2017.22 (2017).

29 Gloster, T. M. *et al.* Hijacking a biosynthetic pathway yields a glycosyltransferase inhibitor within cells. *Nat Chem Biol* **7**, 174-181, doi:10.1038/nchembio.520 (2011).

30 Liu, C. & Li, J. O-GlcNAc: A Sweetheart of the Cell Cycle and DNA Damage Response. *Front Endocrinol (Lausanne)* **9**, 415, doi:10.3389/fendo.2018.00415 (2018).

31 Tan, E. P., Caro, S., Potnis, A., Lanza, C. & Slawson, C. O-linked N-acetylglucosamine cycling regulates mitotic spindle organization. *J Biol Chem* **288**, 27085-27099, doi:10.1074/jbc.M113.470187 (2013).

32 Chen, C. H. *et al.* Characterization of Cep85 - a new antagonist of Nek2A that is involved in the regulation of centrosome disjunction (vol 128, pg 3290, 2015). *Journal of Cell Science* **128**, 3837-3837, doi:10.1242/jcs.180463 (2015).

33 Qin, K. *et al.* Quantitative Profiling of Protein O-GlcNAcylation Sites by an Isotope-Tagged Cleavable Linker. *ACS Chem Biol*, doi:10.1021/acschembio.8b00414 (2018).

34 Woo, C. M. *et al.* Mapping and Quantification of Over 2000 O-linked Glycopeptides in Activated Human T Cells with Isotope-Targeted Glycoproteomics (Isotag). *Mol Cell Proteomics* **17**, 764-775, doi:10.1074/mcp.RA117.000261 (2018).

35 Ramakrishnan, P. *et al.* Activation of the transcriptional function of the NF-kappaB protein c-Rel by O-GlcNAc glycosylation. *Sci Signal* **6**, ra75, doi:10.1126/scisignal.2004097 (2013).

36 Tian, J. *et al.* O-GlcNAcylation Antagonizes Phosphorylation of CDH1 (CDC20 Homologue 1). *J Biol Chem* **291**, 12136-12144, doi:10.1074/jbc.M116.717850 (2016).

37 Lane, H. A. & Nigg, E. A. Antibody microinjection reveals an essential role for human polo-like kinase 1 (Plk1) in the functional maturation of mitotic centrosomes. *J Cell Biol* **135**, 1701-1713, doi:10.1083/jcb.135.6.1701 (1996).

38 Sumara, I. *et al.* Roles of polo-like kinase 1 in the assembly of functional mitotic spindles. *Curr Biol* **14**, 1712-1722, doi:10.1016/j.cub.2004.09.049 (2004).

39 Li, J. *et al.* An Isotope-Coded Photocleavable Probe for Quantitative Profiling of Protein O-GlcNAcylation. *ACS Chem Biol*, doi:10.1021/acschembio.8b01052 (2019).

40 Alfaro, J. F. *et al.* Tandem mass spectrometry identifies many mouse brain

O-GlcNAcylated proteins including EGF domain-specific O-GlcNAc transferase targets. *Proc Natl Acad Sci U S A* **109**, 7280-7285, doi:10.1073/pnas.1200425109 (2012).

41 Yang, W. H. *et al.* Modification of p53 with O-linked N-acetylglucosamine regulates p53 activity and stability. *Nat Cell Biol* **8**, 1074-1083, doi:10.1038/ncb1470 (2006).

42 Pellegrini, M. *et al.* Autophosphorylation at serine 1987 is dispensable for murine Atm activation in vivo. *Nature* **443**, 222-225, doi:10.1038/nature05112 (2006).

43 Shiloh, Y. & Ziv, Y. The ATM protein kinase: regulating the cellular response to genotoxic stress, and more. *Nat Rev Mol Cell Biol* **14**, 197-210 (2013).

44 Silk, A. D., Holland, A. J. & Cleveland, D. W. Requirements for NuMA in maintenance and establishment of mammalian spindle poles. *J Cell Biol* **184**, 677-690, doi:10.1083/jcb.200810091 (2009).

45 Kong, X. *et al.* Cohesin associates with spindle poles in a mitosis-specific manner and functions in spindle assembly in vertebrate cells. *Mol Biol Cell* **20**, 1289-1301, doi:10.1091/mbc.E08-04-0419 (2009).

46 Wang, Z. *et al.* Extensive crosstalk between O-GlcNAcylation and phosphorylation regulates cytokinesis. *Sci Signal* **3**, ra2, doi:10.1126/scisignal.2000526 (2010).

47 Magescas, J. *et al.* Spindle pole cohesion requires glycosylation-mediated localization of NuMA. *Sci Rep* **7**, 1474, doi:10.1038/s41598-017-01614-6 (2017).

48 Liu, D., Davydenko, O. & Lampson, M. A. Polo-like kinase-1 regulates kinetochore-microtubule dynamics and spindle checkpoint silencing. *J Cell Biol* **198**, 491-499, doi:10.1083/jcb.201205090 (2012).

49 Li, J. *et al.* MYPT1 sustains centromeric cohesion and the spindle-assembly checkpoint. *J Genet Genomics* **40**, 575-578, doi:10.1016/j.jgg.2013.08.005 (2013).

50 Li, J. *et al.* Phosphorylation of Ataxin-10 by polo-like kinase 1 is required for cytokinesis. *Cell Cycle* **10**, 2946-2958, doi:15922 [pii] (2011).

492 **Figure Legends**

493 **Figure 1. Elevated O-GlcNAc levels leads to aberrant centrosome separation via**

494 **PLK1.** (A) HeLa cells were treated with TMG, BI2536 or TMG + BI2536, then

495 stained with anti-γ-tubulin antibodies and DAPI. Scale bar, 10 μM. (B) Quantitation

496 of inter-centrosomal distances in (A). More than 25 cells were counted for each

497 experiment. The data represent mean ± S. D. of three independent experiments.

498 Asterisks indicate significant difference as determined by t-test (p1-2=0.005,

499 p2-4=0.008). (C) Quantitation of percent of cells with separated centrosomes in (A).

500 Asterisks indicate significant difference as determined by t-test (p1-2=0.02,

501 p2-4=0.02)

502

503 **Figure 2. OGT interacts with the central region of MYPT1.** (A) Recombinant

504 GST-OGT proteins were incubated with HA-MYPT1-transfected cell lysates. (B)

505 His-OGT and GST-MYPT1 proteins were incubated together and then subject to

506 pulldown assays as indicated. (C) A diagram showing MYPT1 constructs used in this

507 study. Full-length (FL), F1(1-306), F2(297-600), F3(586-901) and F4(886-1030) were

508 previously described [24]. 4A denotes T577AS585AS589AS601A. (D) Recombinant

509 GST-MYPT1-FL, F1, F2, F3 and F4 proteins were purified from bacteria, and

510 incubated with extracts from 293T cells transfected with Myc-OGT. Asterisks

511 demarcate corresponding proteins.

512

513 **Figure 3. MYPT1 is O-GlcNAcylated at T577, S585, S589 and S601.** (A-D)
514 Electron Transfer Dissociation (ETD) mass spectrometry combined with
515 chemo-enzymatic labeling identified that T577S585 S589S601 are O-GlcNAcylated
516 [33].
517
518 **Figure 4. O-GlcNAcylation of MYPT1 antagonizes CDK1-dependent**
519 **phosphorylation at S473.** (A) MYPT1-WT and 4A plasmids together with
520 Myc-OGT or empty vectors were transfected into 293T cells and then blotted with
521 antibodies indicated. (B) Cells were transfected with HA-MYPT1-WT or 4A plasmids,
522 and then the lysates were IBed with antibodies indicated. (C) Cells were treated with
523 Noc, or Noc with Ro-3306 for the time indicated. (D) HeLa cells were transfected
524 with HA-MYPT1, treated or untreated with 5S-G (OGT inhibitor). (E) Cells were
525 treated with Noc, or Noc + 5S-G. (F) Cells were transfected with MYPT1-WT
526 plasmids, and then treated with Noc, or Noc plus TMG + Glu as indicated.
527
528 **Figure 5. O-GlcNAcylation of MYPT1 attenuates the interaction between**
529 **MYPT1 and PLK1.** (A) 293T cells were transfected with Flag-PLK1 and
530 HA-MYPT1, treated or not treated with Noc, TMG + Glu, respectively, then subject
531 to IP and IB as indicated. (B) GST-PLK1-PBD proteins were purified from bacteria.
532 Cells were transfected with HA-MYPT1-WT or 4A, then the cell lysates were subject
533 to GST-PLK1-PBD pulldown assays. (C) Cells were transfected with FLAG-PLK1

534 together with HA-MYPT1-WT or 4A, then subject to IP and IB as indicated. (D)
535 Cells were transfected with HA-MYPT1-WT or 4A, and then cell extracts were
536 utilized in His-PLK1 pulldown assays.
537
538 **Figure 6. O-GlcNAcylation of MYPT1 promotes PLK1 activity.** (A)
539 IP-phosphatase assays. U2OS cells were transfected with Flag-MYPT1, synchronized
540 to mitosis with Noc, then treated with TMG + Glu or left untreated. The anti-Flag
541 immunoprecipitates were then incubated with recombinant His-PLK1. (B)
542 IP-phosphatase assays using the MYPT1-WT and -4A mutants without Noc
543 treatment.
544
545 **Figure 7. MYPT1 overproduction overrides the centrosome disjunction defects**
546 **induced by TMG** (A) Lenti viruses encoding vectors or sh*MYPT1* was introduced
547 into HeLa cells, together with HA-MYPT1-WT or -4A plasmids. The cellular lysates
548 were IBed with the antibodies indicated. (B) Cells in (A) were subject to indirect IF
549 using the antibodies indicated. (C) Quantitation of percent of cells with separated
550 centrosomes in (B). Asterisks indicate significant difference as determined by t-test
551 (p1-2=0.0002, p2-3=0.22, p2-4=0.001). (D) We propose that MYPT1 is
552 O-GlcNAcylated at T577 S585 S589 S601, which antagonizes CDK1-dependent
553 phosphorylation at S473 and MYPT1-PLK1 interaction. By disjoining PLK1 from the

554 MYPT1/PP1cβ complex, PLK1 activity is elevated, thus promoting centrosome

555 separation.

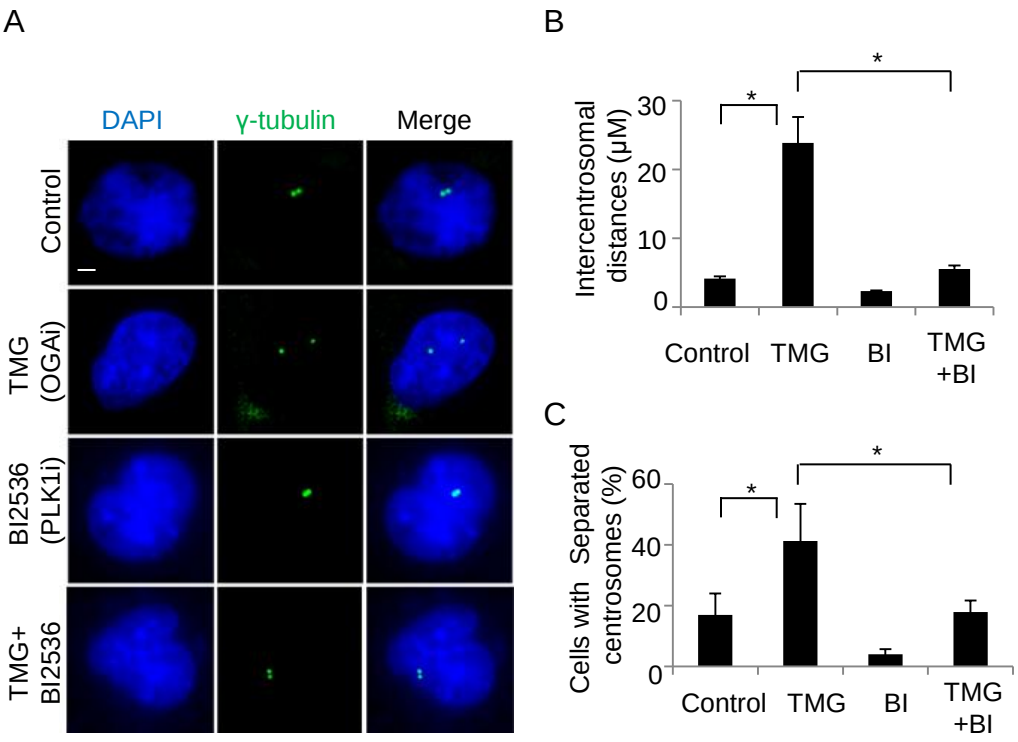
A
DAPI
γ-tubulin
Merge
Control
TMG (OGAi)
BI2536 (PLK1i)
TMG+ BI2536
B
Intercentrosomal distances (μM)
30
20
10
0
*
*
Control
TMG
BI
TMG +BI
C
Cells with Separated centrosomes (%)
60
40
20
0
*
*
Control
TMG
BI
TMG +BI

Figure 1

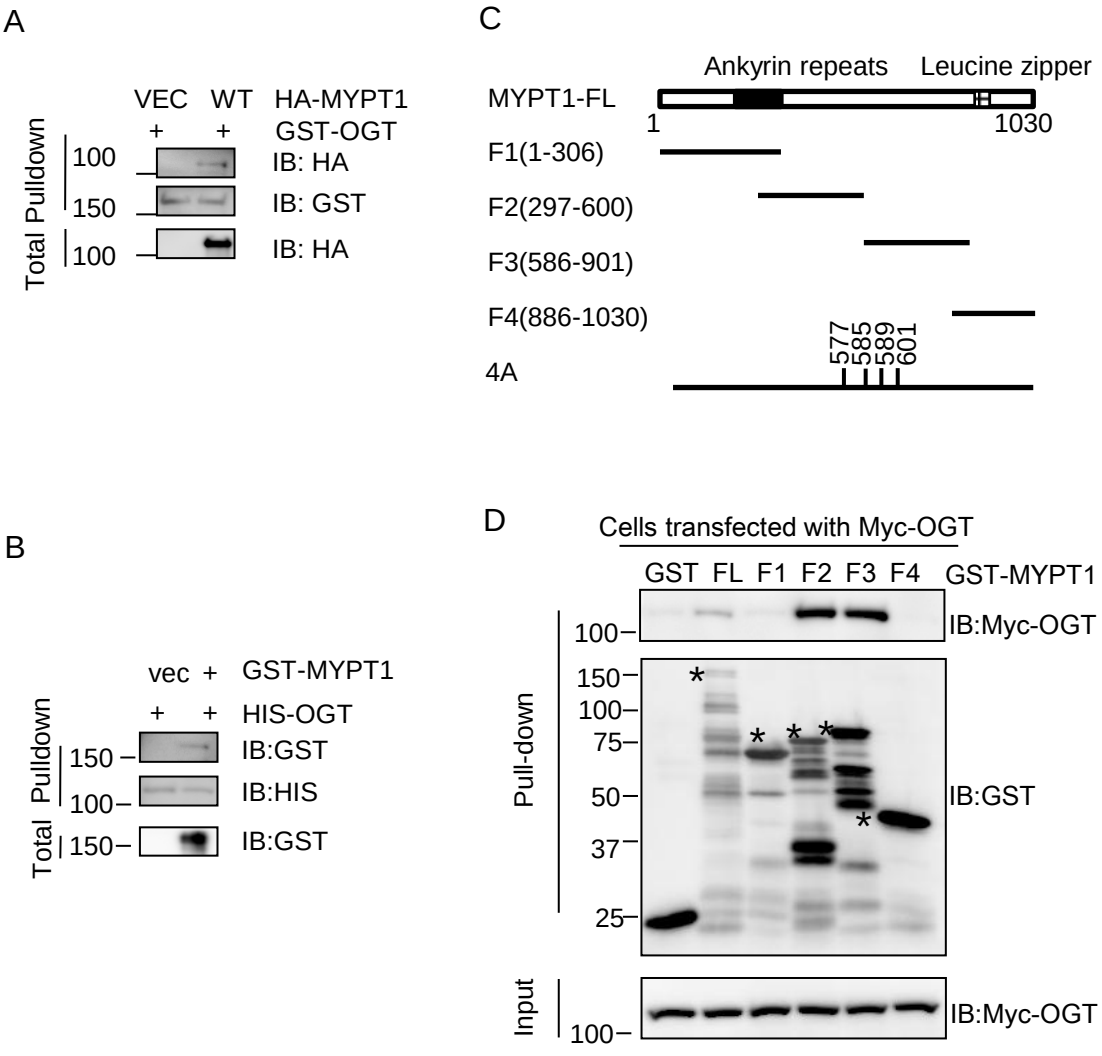
A
VEC WT HA-MYPT1
+ + GST-OGT
Total Pulldown
100
150
100
IB: HA
IB: GST
IB: HA
B
vec + GST-MYPT1
+ + HIS-OGT
Pulldown
150
100
IB:GST
IB:HIS
Total
150
IB:GST
C
Ankyrin repeats
Leucine zipper
MYPT1-FL
1
1030
F1(1-306)
F2(297-600)
F3(586-901)
F4(886-1030)
4A
577
585
589
601
D
Cells transfected with Myc-OGT
GST FL F1 F2 F3 F4 GST-MYPT1
IB:Myc-OGT
Pull-down
100
150
100
75
50
37
25
IB:GST
Input
100
IB:Myc-OGT

Figure 2

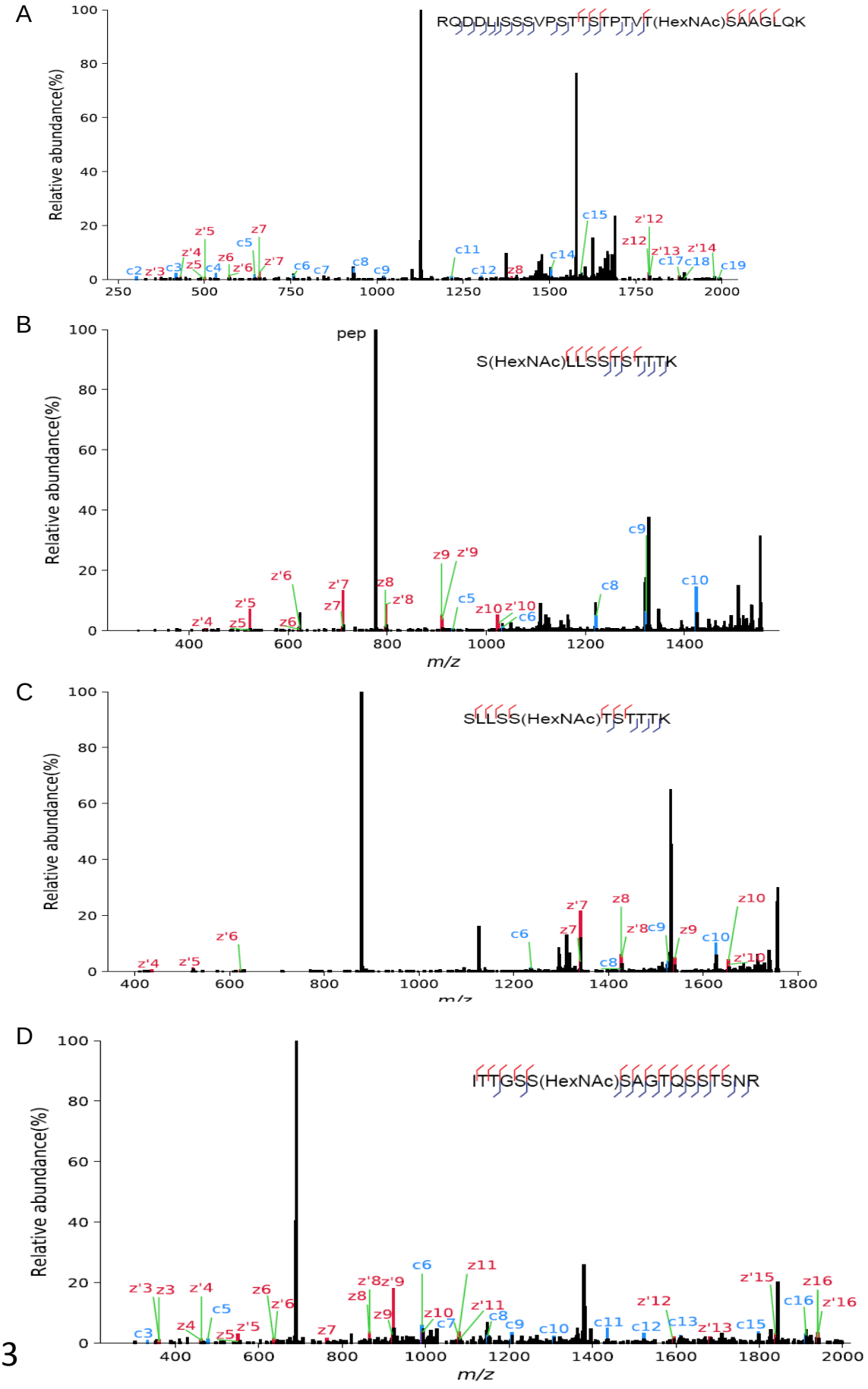
A
RQDDLISSSVPSTTSTPTVT(HexNAc)SAAGLQK
Relative abundance(%)
B
pep
S(HexNAc)LLSSTSTTTK
Relative abundance(%)
m/z
C
SLLSS(HexNAc)TSTTTK
Relative abundance(%)
D
ITTGSS(HexNAc)SAGTQSSTSNR
Relative abundance(%)
m/z

Figure 3

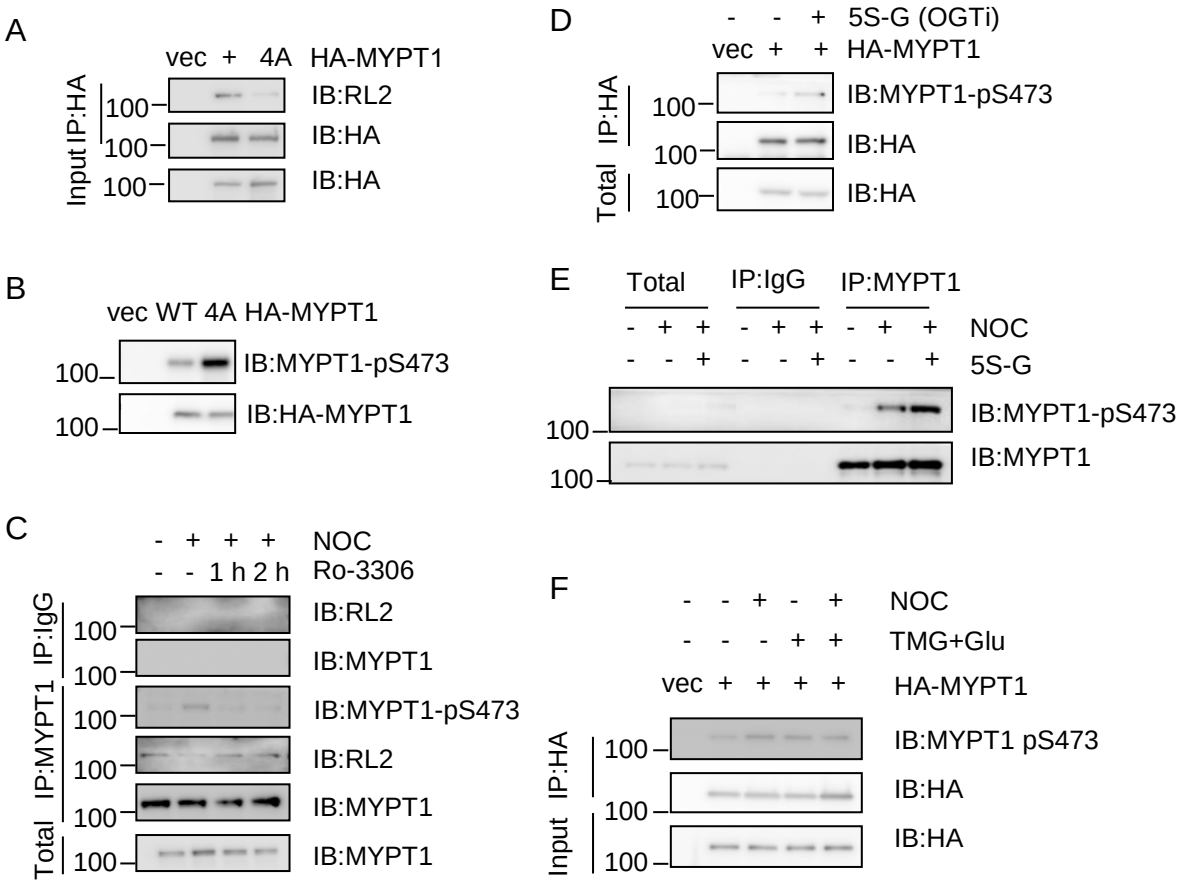
A
vec + 4A HA-MYPT1
Input IP:HA
100
IB:RL2
100
IB:HA
100
IB:HA
B
vec WT 4A HA-MYPT1
100
IB:MYPT1-pS473
100
IB:HA-MYPT1
C
- + + + NOC
- - 1 h 2 h Ro-3306
IP:IgG
IP:MYPT1
Total
100
IB:RL2
100
IB:MYPT1
100
IB:MYPT1-pS473
100
IB:RL2
100
IB:MYPT1
100
IB:MYPT1
D
- - + 5S-G (OGTi)
vec + + HA-MYPT1
Total IP:HA
100
IB:MYPT1-pS473
100
IB:HA
100
IB:HA
E
Total
IP:IgG
IP:MYPT1
- + + - + + - + + NOC
- - + - - + - - + 5S-G
100
IB:MYPT1-pS473
100
IB:MYPT1
F
- - + - + NOC
- - - + + TMG+Glu
vec + + + + HA-MYPT1
Input IP:HA
100
IB:MYPT1 pS473
100
IB:HA
100
IB:HA

Figure 4

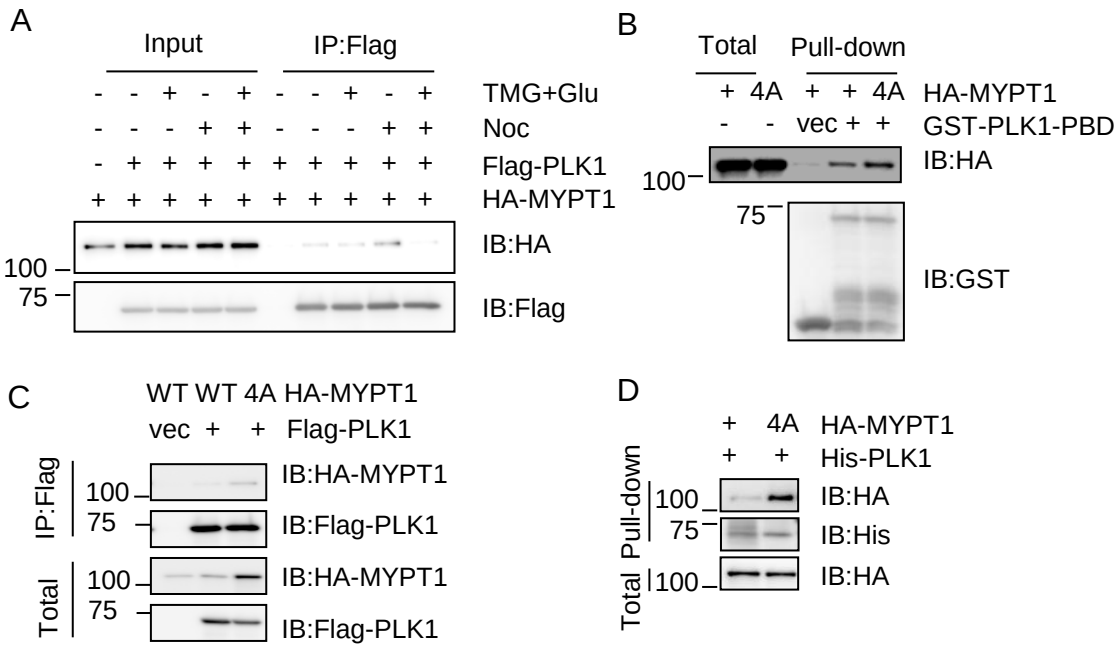
A
Input
IP:Flag
TMG+Glu
Noc
Flag-PLK1
HA-MYPT1
IB:HA
IB:Flag
100
75
B
Total
Pull-down
HA-MYPT1
GST-PLK1-PBD
IB:HA
IB:GST
100
75
C
WT WT 4A HA-MYPT1
vec
Flag-PLK1
IP:Flag
Total
IB:HA-MYPT1
IB:Flag-PLK1
100
75
D
HA-MYPT1
His-PLK1
Pull-down
Total
IB:HA
IB:His
100

Figure 5

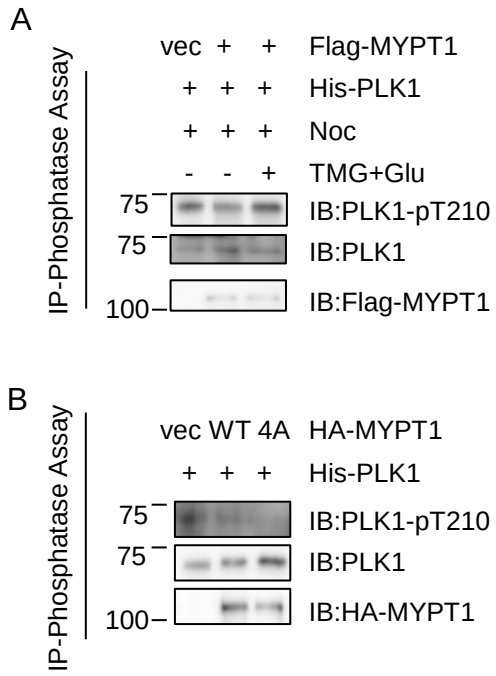
A
IP-Phosphatase Assay
vec + + Flag-MYPT1
+ + + His-PLK1
+ + + Noc
- - + TMG+Glu
75
IB:PLK1-pT210
75
IB:PLK1
100
IB:Flag-MYPT1
B
IP-Phosphatase Assay
vec WT 4A HA-MYPT1
+ + + His-PLK1
75
IB:PLK1-pT210
75
IB:PLK1
100
IB:HA-MYPT1

Figure 6

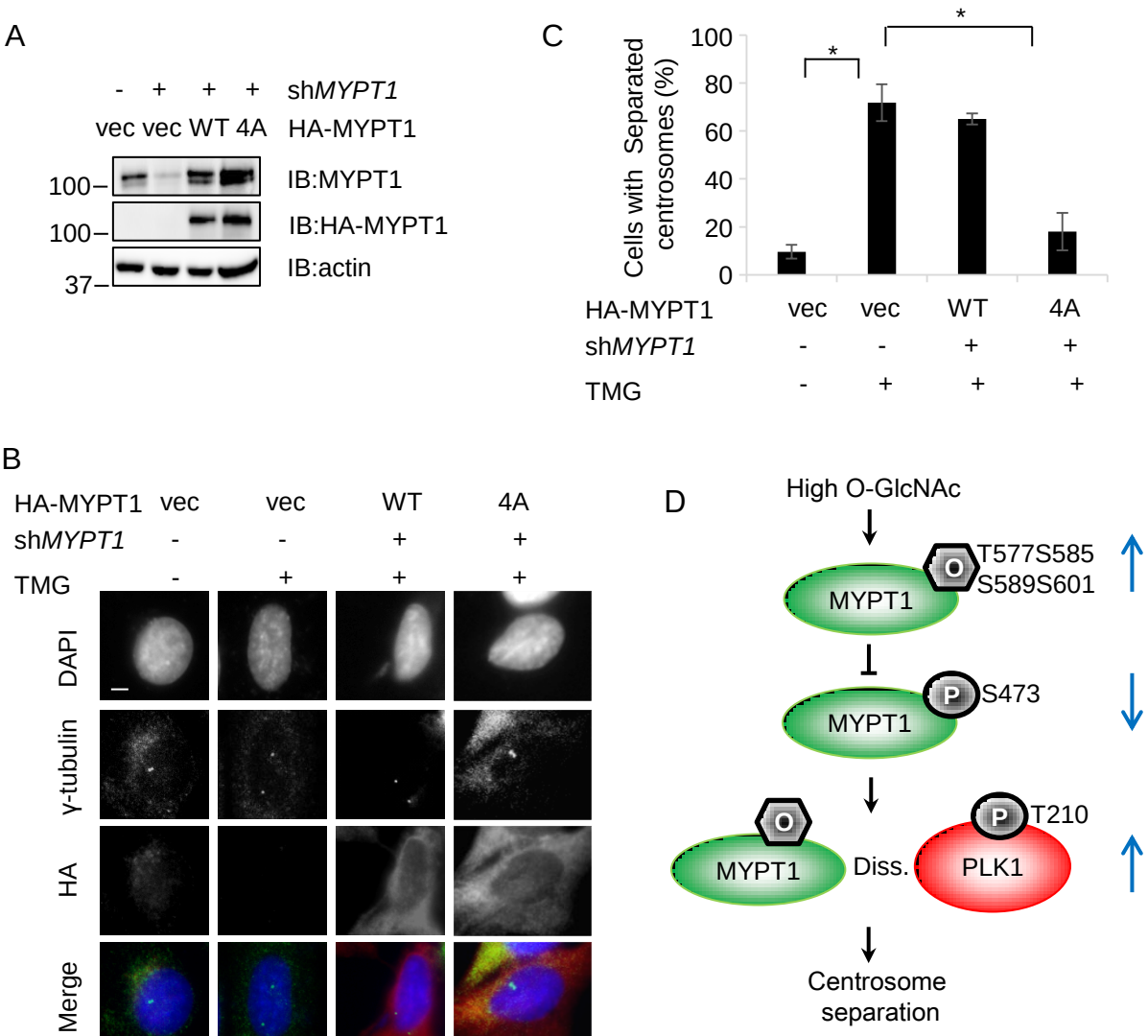
A
- + + + shMYPT1
vec vec WT 4A HA-MYPT1
100–
IB:MYPT1
100–
IB:HA-MYPT1
37–
IB:actin
C
Cells with Separated centrosomes (%)
100
80
60
40
20
0
*
*
HA-MYPT1 vec vec WT 4A
shMYPT1 - - + +
TMG - + + +
B
HA-MYPT1 vec vec WT 4A
shMYPT1 - - + +
TMG - + + +
DAPI
γ-tubulin
HA
Merge
D
High O-GlcNAc
MYPT1
T577S585
S589S601
MYPT1
S473
MYPT1
Diss.
PLK1
T210
Centrosome separation

Figure 7